IEEE Access
Multidisciplinary | Rapid Review | Open Access Journal

Received 28 June 2024, accepted 5 July 2024, date of publication 12 July 2024, date of current version 23 July 2024.

Digital Object Identifier 10.1109/ACCESS.2024.3427386

RESEARCH ARTICLE

IoT-Driven Microseismic Sensing System and Monitoring Platform for Landslide Detection

P. K. INDUKALA, U. G. GOSH, AND MANEESHA VINODINI RAMESH, (Senior Member, IEEE)
Center for Wireless Networks & Applications (WNA), Amrita Vishwa Vidyapeetham, Amritapuri, India

Corresponding author: P. K. Indukala (indukalapk@am.amrita.edu)

This work was supported in part by the Ministry of Earth Sciences (MoES), Government of India, and Sikkim State Disaster Management Authority (SSDMA) under the project titled "Advancing Integrated Wireless Sensor Networks for Real-Time Monitoring and Detection of Disasters;" and in part by Amrita Vishwa Vidyapeetham.

ABSTRACT Landslides pose a significant threat to human life and infrastructure, causing extensive damage and fatalities. Effective monitoring and dissemination of early warnings of imminent landslides are constrained by a lack of precise spatial and temporal information on landslide triggers and uncertainties of the factors that lead to such events. This paper addresses these issues by presenting an Internet of Things (IoT)- driven platform designed to capture microseismic vibrations in landslide-prone areas. The proposed system aims to provide insights into the onsets of hazardous landslides, particularly those stimulated by heavy rainfall and earthquakes. This treatise utilizes a microseismic smart sensing system with geophone sensors (SM-s nodes) which continuously records and transmits real-time data on seismic activities associated with potential landslides, enabling timely propagation of early warnings. The proffered system's ability to acquire and characterize microseismic signals was systematically validated through an integrated set of landslide laboratory experiments, outdoor field trials, and real-world deployment in Chandmari located in the State of Sikkim, India, situated in the North-Eastern Himalayan region. Furthermore, the paper provides an in-depth analysis of the historical microseismic activities, differentiating them from ambient noises such as pedestrian and vehicular movements and slope instabilities triggered by rainfall and earthquakes. The system's performance was evaluated during three real-world events: two earthquakes and an instance of rainfall precipitation. This study explored the time and frequency characteristics as well as the variations of ground motion parameters during recorded slope instabilities. A comparative analysis of existing microseismic monitoring approaches was also conducted to assess the effectiveness of the proposed system. The insights gained from this work were instrumental for the development of decision models capable of identifying precursory microseismic activities precedent to imminent landslides, towards safeguard of lives and property damage.

INDEX TERMS Early warning systems, geophones, IoT platform, landslides, microseismic signals, system design, signal processing, wireless sensor networks.

I. INTRODUCTION

Landslides pose significant threats to both human lives and infrastructure, as they involve the unpredictable disruptive movements of soil, rock, and other materials under the force of gravity [1]. Recent research has pinpointed the staggering impact of landslides, with over 72,000 fatalities and USD 11.5 billion in damages, globally, recorded between 1900 and 2022 [2], [3]. Almost 75 % of these deadly incidents transpired in Asian nations, with a notable concentration in the Himalayan regions of northern India [4].

Landslide events are triggered by various factors, such as heavy rainfall, earthquakes, and anthropogenic activities, severally or in tandem [5], [6]. Intense rainfall saturates

The associate editor coordinating the review of this manuscript and approving it for publication was Hosam El-Ocla.

soil and destabilizes natural slopes whereas seismic events weaken soil shear strength that culminate in frequent instances of rapid landslides. Human endeavors such as mining, road and dam construction can disrupt landscapes or weaken soil structures that precipitate landslides. Recurrent stick-slip motion along ruptured surfaces of steep slopes, breakage of soil pipes, strains and displacements due to progressive failure, sudden changes in load distribution along the shear surface due to brittle soil, and seismic forces furnish additional pointers to impending landslides [7], [8].

The Himalayan regions, typified by recent tectonic landslides, linked to rock mass fracturing and uncontrolled road cuttings are characterized by intricate geological compositions, steep gradients, and high topographical ruggedness. These factors, amplified by seismic activity and heavy deluge significantly increase the susceptibility to coseismic landslides [9], [10], [11]. Given these risks, implementation of early warning systems is crucial for the propagation of timely alerts, propitious to minimized property damage and enhanced communal welfare.

Most early warning systems for rainfall-induced landslides rely on precipitation thresholds, with limited studies investigating the microseismic precursory signals responsible for landslides, especially coseismic landslides [9], [12]. In-situ landslide monitoring entails direct measurement of soil moisture, pore water pressure, and ground deformation using geophysical instruments. Such setups facilitate precise, localized data and real-time monitoring or geological transitions [13], [14], [15]. However, the preceding options are pricey, afford limited spatial coverage, and rely on communication technologies with lower data rates, which are ill-suited for detailed microseismic monitoring [1], [16], [17]. Affordable low-power sensors offering spatial information with high resolution and minimal latency, are the preferred attributes of an ideal intelligent Landslide Early Warning system [1], [18].

Traditional geodetic surveying methods are inefficient and require skilled workers whereas remote sensing techniques lack real-time resolution, obligatory for automated data analysis [19]. Geophysical monitoring methods furnish valuable information on subsurface slope activities and precursory failure conditions [15], [20], [21], [22]. Standardized automated techniques for large-scale spatial analysis using these approaches is challenging in fragile Himalayan terrains. Nevertheless, these methods are expensive and mandate specialized equipment and domain expertise, exacerbating implementation in disaster-prone areas [20].

The Himalayan region is characterized by shearing rocks and highly jointed geologic formations, undergoing multiple phases of deformation, continuing to which move at rates ranging from a few millimeters to several centimeters per year [9]. Additionally, drilling activities in these regions could aggravate the vulnerability to landslides and other mass earthly movements. Deep drilling methods are particularly unsuitable due to the risks of borehole collapses, destabilization of hill slopes, and potential landslide triggers. These challenges highlight the critical need for non-invasive techniques to understand subsurface changes of the underlying landslide phenomena effectively. Microseismic monitoring, prompted by geophysical sensors, can detect faint earth tremors effectuating broad spatial coverage and non-invasive sensing of deep subsurface changes, precluding the need for drilling, thereby minimizing environmental disturbances [15].

Microseismic signals precedent to landslide events afford pragmatic precursors apropos slope instabilities or failures, onset by water infiltration, seasonal variations in pore pressure within the soil mass, expansion of micro-cracks, and seismic activities [23], [24], [25], [26], [27], [28], [29], [30]. Identification of pre-trigger signals is inevitable as landslides can occur abruptly. However, the microseismic signals, symptomatic of impending landslides, are relatively weak and vulnerable to noise interferences. Noise interjections creep in from divergent sources- surface or subsurface movements of cracks, terrestrial faults, water infiltration, and anthropogenic excursions. These disturbances obscure targeted seismic signals impeding effective characterization of seismic events associated with landslides, and the site-specific noises [21], [22].

Microseismic sensors integrated with Internet of Things (IoT) technology augment the monitoring of landslides by enabling real-time data collection, which bolster predictive capabilities of monitoring systems, propitious to enhanced safety and resilience of communities in landslide-prone regions. All the same, development of real-time IoT landslide monitoring systems are riddled with challenges. Conventional IoT gadgets are constrained in their ability to acquire, process, and transmit sensor data of higher resolution. These limitations spawn increased development costs, higher energy consumption, and a dependance on centralized data centers [14]. Therefore, there is an exigent need for the development of cost-effective, non-invasive real-time monitoring solutions that acquire multiple microseismic triggers of landslides, to effectuate early warning capability. Such systems in hazardous Himalayan terrains that enable the understanding of subsurface changes over large areas is undubitable. The key requirements for such a system are detailed below.

Microseismic events are typically within the range of natural seismic activity falling below 100 Hertz [31], unlike human/vehicle movements that produce vibrations in higher frequency ranges based on the activity, and environment characteristics [20], [32], [33], [34]. There is a need to capture the microseismic activity beneath the earth's surface, where landslides and earthquakes originate, through precursory signals. The seismic signals associated with landslides often fall under the (0-10) Hz frequency range [20], [35], [36]. For accurate capture of microseismic signals, a data collection system should follow the Nyquist-Shannon sampling theorem, which calls for a sampling rate of at least twice the maximum frequency of the monitored signal [37]. However, a much higher sampling rate, typically ten times the maximum signal frequency, is recommended to capture subtle microseismic activities. Contemporary ealy warning systems are often designed for real-time lower data rates processing and transmission [20], [38]. Therefore, a system is needed that can acquire microseismic signals in real-time, at high sampling rates from multiple triggers, sustain harsh environments, with an extended service lifetime.

Based on these requirements, the key research problem can be stated as- how to effectively capture early triggers of landslides in real-time in resource-constrained regions, using microseismic monitoring approaches to save lives and abate property damage.

Major contributions of this investigation are summarized as follows:

- Introduction of an *IoT-driven platform* with tailor-made components for acquisition and seamless data transmission of subterranean microseismic vibrations in the face of heavy rainfall and earthquakes, across multiple edges and cloud.
- Development of a *Smart Microseismic Sensing system*, incorporating geophone sensors, referred to as SM-s nodes, for incessant capture, record and transmission of real-time data from landslide-prone areas.
- Empirical assessment, validation and verification, via *laboratory set-ups and field deployment* of the operational capabilities of the proffered smart microseismic sensing nodes.
- *Implementation of the IoT-driven microseismic smart sensing system* in the Himalayan region characterized by active tectonics and frequent heavy rainfall, where both landslides and earthquakes are common occurrences, facilitating the continuous real-time transmission of the earth's vibrational data.
- Comprehensive *analysis of historical microseismic data*, from multiple SM-s nodes deployed at the Chandmari site, focused on slope instabilities actuated by precipitation and seismic tremors.

This monitoring system was deployed at Chandmari, in the East Sikkim district of the State of Sikkim, within the North-eastern Himalayan region [subsection III-D].

A. PAPER OUTLINE

The rest of this paper is organized as follows: Section II, delves into architectural details of the microseismic signal monitoring platform for landslide detection and early warning systems. Section III surmises the methods used for validation of the proposed microseismic sensing system, via laboratory setups, implementation in real-world operational scenarios and data processing methods for microseismic signal characterization. Section IV describes the results and discussions on the analysis of microseismic signals acquired from the proffered system. Section V provides a comparison of the proposed system with existing systems pertinent to microseismic landslide monitoring. Conclusions and directions of future research are covered in section VI.

II. MICROSEISMIC SIGNAL MONITORING PLATFORM

This section discusses the proposed IoT-driven microseismic signal monitoring platform, suitable for large-scale spatiotemporal monitoring, real-time data acquisition, and classification of microseismic signals to identify imminent landslides. The key components of the proposed monitoring platform are detailed herein.

A. SENSORS AT EDGE

The proposed system was conceived to provide a low-cost solution for effective capture of microseismic activity beneath the earth's surface, which emanate landslide pre-triggers. Extant sensing instruments listed in Table 1 are capable of detecting subtle microseismic signals. The table acquaints parameters such as bandwidth capability, number of axes, weight, power requirements, and cost of these seismic instruments. Notably, the listed seismometers are active, heavy, and expensive, while the moderately priced active or passive accelerometers, are capable of only detecting surface movements. Geophones stand out as the optimal choice due to their resilience to harsh environments and their ability to detect ultra-low frequency bands and low-magnitude vibrations [39]. Low-cost, passive, and lightweight geophones were selected for this study, for their ease of deployment and maintenance. To further enhance their functionality, geophones can be outfitted with IoT capabilities, enabling real-time data transmission to the cloud, augmenting their effectiveness in capturing and relaying valuable seismic information.

TABLE 1. List of seismic sensors.

Seismic Sensors	Bandwidth	Axes	Weight	Power	Cost
Strong Motion Accelerometer	(0.1-100) Hz	1,2,3	25.0 Kg	Active, Passive	Intermediate
Force Balanced Accelerometer	(DC-100) Hz	1,2,3	3.0 Kg	Active	Intermediate
Strong-motion Force Feedback Accelerometer	(DC-100) Hz	1,3	2.05 Kg	Active	Intermediate
Short Period Seismometer	(4.5-315) Hz	1,2,3	20.0 Kg	Active	High
Short Period Seismometer	(1-50) Hz	1,2,3	25.0 Kg	Active	High
Weak Motion Broadband Seismometer	(0.01-50) Hz	3	19.0 Kg	Active	High
Broadband Seismometer	(0.033-50) Hz	3	7.5 Kg	Active	High
Geophone (10 Hz)	(0- 250) Hz	3	0.85 Kg	Passive	Low
Geophone (30 Hz)	(0-500) Hz	3	0.85 Kg	Passive	Low

The proposed smart microseismic sensing system employed geophone sensors to continuously capture, record, and transmit real-time vibrational data on microseismic events occurring in landslide-prone regions, as shown in Figure 1. A geophone, functioning as a ground motion transducer, generates an analog differential voltage output across its terminals, which is directly proportional to the velocity of ground vibrations induced by the surrounding medium. These compact, self-powered sensors offer a flat frequency response in velocity, within a specific frequency

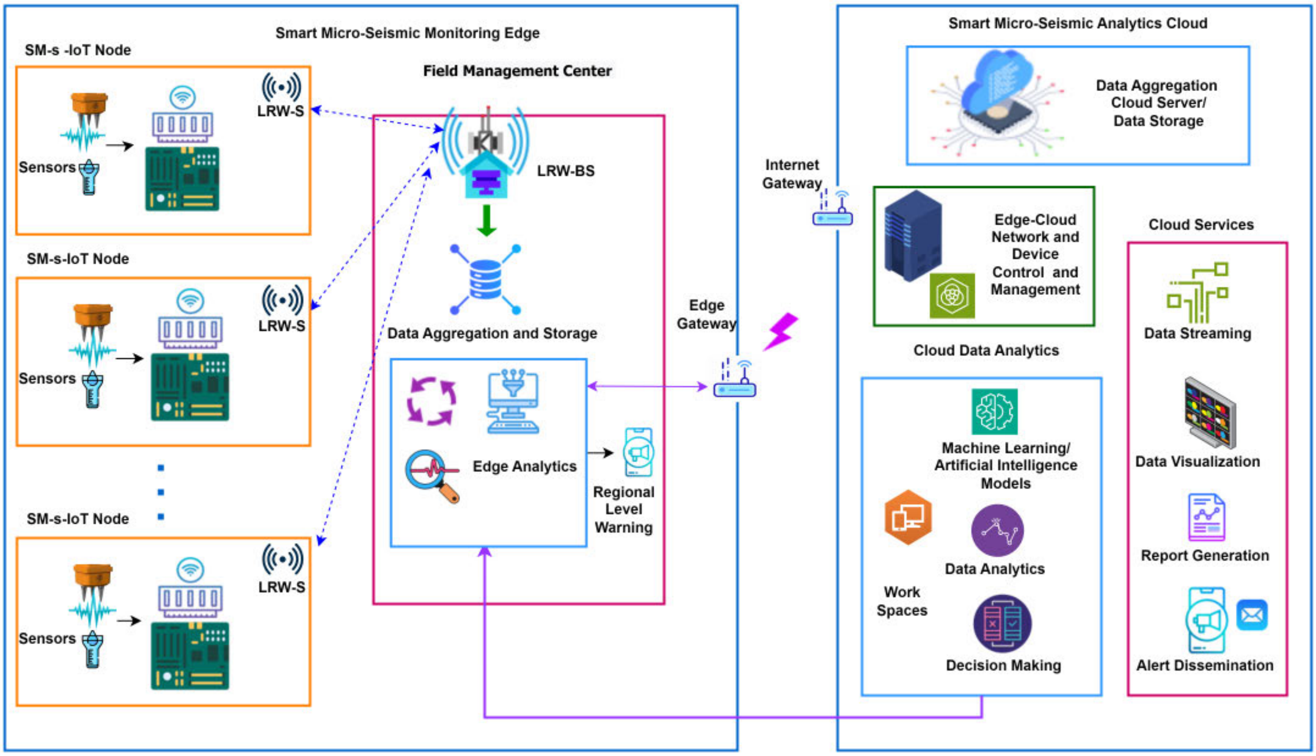

FIGURE 1. Microseismic signal monitoring architectural framework enabling the capture and transmission of vibrational data from Smart microseismic IoT Devices across heterogeneous data networks, facilitating detection and monitoring of microseismic activity in landslide-prone regions.

range above their resonant frequencies and attenuate frequencies below them, rendering them well-suited for the measurement of ground velocity.

For recording the earth's ground vibrations, multiple tri-axial geophones equipped with three terminals were utilized: Horizontal-1 (H1), Horizontal-2 (H2), and Vertical (V3) axes, corresponding to waveform propagation in the X (North-South), Y (East-West), and Z (Up-Down) directions, respectively [14], [22]. Geophones with resonant frequencies of 10 Hz and 30 Hz were strategically placed at locations mentioned in subsection III-D, to examine signal patterns, associated spectral range of gradual subsurface movements, and rapid fractural/ slip surface movements within the landslide mass, taking into account the trade-offs discussed in section I.

Standard tipping bucket gauges within a rain-gauge system for the measurement of rainfall intensity were also employed, in tandem with the geophone sensors. This strategic integration enabled detailed comparison of rainfall variations and a study of the pretrigger patterns recorded by the geophones, in landslide-prone regions, during periods of intense rainfall and earthquake tremors.

B. SMART MICROSEISMIC MONITORING EDGE (SM-S NODES)

The Smart Microseismic Monitoring Edge forms the heart of the architecture, featuring highly specialized microseismic sensors as shown in Figure 1. These sensors operate in synergy with supporting components like microcontrollers, signal conditioning boards, communication modules, power supply units, batteries, solar panels, among other peripherals. This system enables local data processing and initial decision-making, instead of centralized processing to ensure swift responses. The strategically deployed system collects, stores, transmits, and analyzes ground vibrations related to microseismic activities, in landslide prone areas.

1) DATA ACQUISITION HARDWARE PLATFORM

A custom data acquisition hardware was designed for the precise acquisition of signals from the geophone sensors, facilitating accurate measurement of microseismic activities, as represented in Figure 2. This hardware was constituted of the following components: a pre-conditioning filter unit, an amplification and differential-to-single-ended conversion unit, and a power supply unit for essential support. The terminals originating from the geophone sensors were configured differentially. Paired outputs from each geophone terminal were initially directed into a pre-conditioning unit, comprised of preamplifiers and filtering systems, as shown in Figure 2.

This stage serves to amplify the delicate seismic vibrations detected by the geophones and effectively eliminate Radio Frequency (RF) and other high-frequency noise sources. Noise reduction was accomplished through the

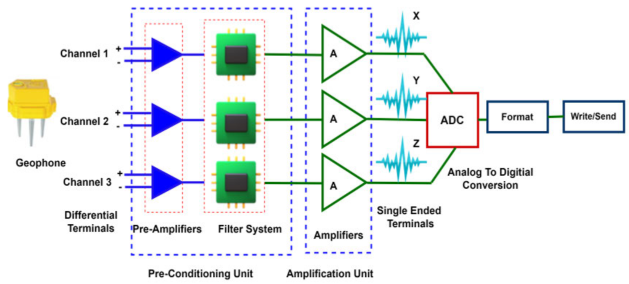

FIGURE 2. Geophone data acquisition process.

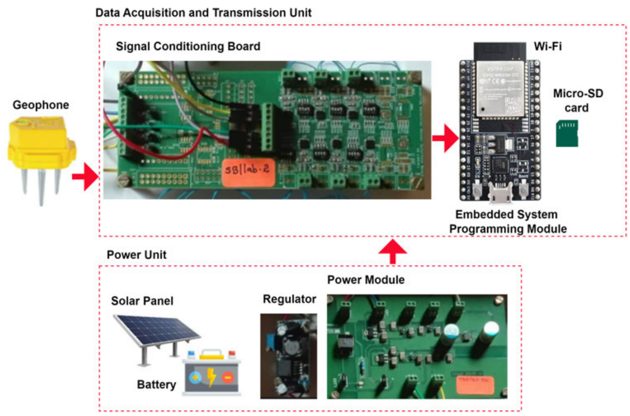

FIGURE 3. Microseismic sensing node for geophones.

implementation of a first-order Resistor-Capacitor- Low Pass Filter (RC-LPF) with an anti-aliasing cutoff at 156 Hz. The first-order passive Low Pass Filter (LPF) was chosen for its cost-effectiveness and durability in challenging environments. This decision was in tune with the objective of developing an affordable sustainable solution for the continuous acquisition and monitoring of microseismic signals. Increasing the filter order would impose greater circuit complexity that potentially calls for expensive active filters, validating the choice of a passive first-order LPF.

Following the geophone signal's pre-conditioning phase, the filtered signals are routed into instrumentation amplifiers, outfitted with variable gain adjustment options. The precision of this gain was finely tuned to the desired level via a network of resistors, controlled by a Printed Circuit Board (PCB)-mountable switch. Subsequent to the fine-tuning stage, single-ended outputs from the three geophone terminals were seamlessly directed toward analog-to-digital conversion (ADC) units. The dig of the three outputs were formatted to facilitate storage within Secure Digital (SD) cards and subsequent transmission stages. It is imperative to comprehend that this data acquisition hardware is the key for the accurate capture of microseismic vibrations from geophones, ensuing in a reliable and robust measurement system.

Programming modules in Figure 3 are energy-efficient systems-on-a-chip solutions equipped with built-in Wi-Fi capabilities and ADC input channels of 12-bit resolution. The entire system transforms into a cost-effective IoT-enabled configuration known as a *Smart Microseismic Sensing and Monitoring edge or SM-s nodes* within the proposed sensing system. The proposed design adopted solar-powered renewable energy sources via solar panels, to conserve energy. The power system was comprised of renewable energy sources such as solar panel, which is the main source, and the local power grid (AC socket power), both of which were interfaced to a battery. The charge controller unit ensures that power was properly fed to energize lead acid batteries. Context aware energy management techniques, for effective power consumption in edge sensing systems were incorporated as outlined in [40], which extends the system lifetime.

Sensitivity of the proffered microseismic data acquisition system using a N-bit ADC (here,N=12) with a full-scale range can be calculated as shown in eqn.1:

$$S_{\text{ADC}} = \frac{V_{\text{ADC}}}{(2^N - 1)} \approx \frac{V_{\text{ADC}}}{(2^{12} - 1)} \approx 0.000805 \text{ V/bit}. \tag{1}$$

where V_{ADC} is the output ADC value. Given that the sensitivity of the geophone is S_{Sensor}, the overall sensitivity of the system is defined in eqn.2:

$$S_{\text{System}} = \frac{S_{\text{ADC}}}{S_{\text{Sensor}}} \approx \frac{0.000805 \text{ V/bit}}{28.8 \text{ V/(m/s)}} \approx 2.8 \times 10^{-5} \text{ m/s/bit}. \tag{2}$$

2) FIRMWARE DEVELOPMENT

The geophone data acquisition firmware was developed within the open-source Arduino Integrated Development Environment (version 1.6.13), for in-depth exploration of subsurface movements within Sikkim's challenging terrain, and capture of microseismic signals. The effective capture of microseismic signals, mandate employment of high sampling rates, at least ten times the maximum signal frequency, as discussed in section I. Lower data rates pertain to frequency of acquiring the data at longer intervals, such as one sample per minute or every five minutes, in lieu of incessant acquisition. This can curb the timeliness and resolution of the microseismic data, potentially reducing the effectiveness of monitoring and early warning systems.

Therefore, acquisition of geophone signals at higher data rate of 1 kHz (across three axis or channels) from multiple locations, mentioned in section II-B3 was chosen for comprehension of the intricate subsurface changes beneath the earth's surface and the dynamics of landslides. The proposed data acquisition system for geophones was engineered to record signals at a rate of 1000 samples per second at each channels, and empowered to locally store microseismic data as a means of data back-ups. This sensing concept operated within a holistic framework, constituted of data acquisition, signal amplification, signal preprocessing for high-frequency noise reduction, and data compression modules, all seamlessly integrated into an IoT environment. This multifaceted functionality empowered the sensing system as a highly efficient and versatile edge node.

3) DATA GENERATION

The proposed sensing system generated geophone data that represented ground vibrations evolving from diverse geological processes- rock fracturing, tectonic movements, or slope instabilities, along with the rainfall rates measured by the supportive rain gauges. These parameters collectively offer insights into environmental conditions and seismic activities in landslide-prone areas. In addition, metadata is generated to provide supplementary information for each parameter. The metadata is comprised of timestamps, location coordinates, sensor information, and other pertinent parameters, that enrich the utility of the collected data.

Every sensing node produces significant amounts of data. To store the geophone data every second, from the three channels on an SD card, a minimum storage capacity of approximately 14.4 gigabytes per hour with a data-rate of 4 Mbps is required. Such sizable storage demand compel real-time data transmission. A minimum data-rate of 36 Kbps, is attained by sampling each channel at 1 kHz with a minimum resolution of 12 bits.

C. DATA COMMUNICATION

Given the study region's rugged terrain, discussed in III-D1, an effective communication system is imperative, considering factors such as bandwidth, data rate, frequency, and propagation factors, specific to the deployment site. Traditional cellular network standards, such as Global System for Mobile Communications (GSM), 3G (Third Generation), and 4G (Fourth Generation) stipulates limited bandwidth and lower data rates, rendering them incapable for real-time transmission of extensive geophone-generated data. As 5G (Fifth Generation) technology may not be universally accessible, alternative Low Power Wide Area Network (LPWAN) technologies like Long Range (LoRa) and Narrowband Internet of Things (NB-IoT) were developed for lower data rates that are ill-suited for this purpose.

Given the specific conditions of the deployment area, including dense vegetation and dynamic climatic extremes, Wi-Fi stands out as the optimal choice for real-time transmission of geophone data. Long-range Wi-Fi systems extend connectivity over vast distances, enabling point-to-point or point-to-multipoint connections across ranges of hundred meters to several kilometers [41].

Accordingly, Wi-Fi and long-range Wi-Fi technologies were adopted for intermediate data transmission along with connectivity protocols such as Transmission Control Protocol/Internet Protocol (TCP/IP), and Hypertext Transfer Protocol (HTTP)/ Hypertext Transfer Protocol Secure (HTTPS) to facilitate data transmission with efficiency and scalability. These technologies perfectly match the requirements by extending network coverage to challenging environments, furnishing internet access, and establishing connectivity between remote outlying locations.

Functioning as a Base Station, the Field Management Center (FMC), leverages long-range Wi-Fi technology, is denoted as Long Range Wi-Fi Base Station (LRW-BS). At each location of the SM-s nodes, there are strategically positioned Wi-Fi routers, operating as Access Points in station mode, termed as Long-Range Wireless Wi-Fi stations (LRW-S), along with heterogenous wireless networks [41]. Data from SM-s nodes are seamlessly routed through LRW-S to the FMC via LRW-BS, as shown in Figure 1. This process enables the collection and aggregation of data from SM-s nodes into a local storage/database, where raw sensor data is also stored. FMC facilitates local processing, data analytics, and initial decision-making, bringing intelligence to the edge of the network.

The intermediate processors at the FMC aggregate data from SM-s nodes, enabling regional-scale data analysis and a first level of alert dissemination. FMC also facilitates determination of site-specific thresholds, and event detection to boost efficiency in signal analysis. This strategic step enables the regional-scale analysis of data and the dissemination of initial alerts. The cloud-based edge intelligence algorithms are seamlessly deployed to the processors within the FMC. These algorithms are continuously refined and updated, driven by valuable feedback collected from the field.

D. SMART MICROSEISMIC ANALYTICS CLOUD

1) EDGE-CLOUD NETWORK, EDGE DEVICE CONTROL AND DATA MANAGEMENT

The Smart microseismic Analytics Cloud is comprised of a centralized hub or cloud infrastructure (server) via Internet Gateways for long-term storage (data repository), archiving, and systematic data management. Routers and gateways, operating at edge, and cloud, facilitate end-to-end communication among SM-s nodes, FMCs, and cloud data centers, ensuring dependable data transfer. The edge-cloud network and edge device control are managed at the cloud level by monitoring the status of connected SM-s nodes and the connectivity to the FMC and cloud server. Over-the-air (OTA) updates keep the SM-s nodes secure and up to date with firmware changes (bug fixes and enhancements). Cloud-based device management facilitates the distribution of OTA updates, ensuring that SM-s nodes receive patches and improvements obviating manual intervention.

A data synchronization system in [42] combines data from various landslide deployments into a unified central cloud server. Communication between the sites and the server is established through sockets, allowing the server to receive streaming data from the edge devices and store it in a centralized database, Aggregated Landslide Data [42]. The FMC-Site client system excels at managing reconnections without compromising performance and functionality. The centralized repository enables cross-site analysis, enhancing predictive capabilities for landslide monitoring across multiple locations [42].

2) CLOUD DATA ANALYTICS: GETTING INSIGHTS FROM MICROSEISMIC SIGNALS

The Smart microseismic Monitoring Cloud ensures data durability and seamless accessibility, facilitating its utilization by the adoption of advanced machine learning /artificial intelligence algorithms and data mining techniques [43], [44], [45], [46], [47], [48]. The core objective is to glean valuable insights from the microseismic data originating from diverse locations, for systematic analysis of the landslide signals. Multi-tier signal processing framework, discussed in III-E allows for selective noise removal from various frequency bands, while retaining signal features, fine-tuned to site-specific thresholds for event detection and signal analysis.

The framework is seamlessly integrated into the FMC processors at the edge, empowers the FMC to issue timely alerts and warnings, strengthening its proactive response capabilities. Such an approach significantly reduces the burden on central data centers and cloud resources. This translates to cost-effective and energy-efficient operations, rendering the framework sustainable for long-term monitoring efforts.

3) CLOUD SERVICES

Centralized monitoring at the cloud is facilitated by a dedicated monitoring center which serves as the nexus for real-time streaming of microseismic data originated from diverse locations under surveillance. Its primary mission is to ensure uninterrupted monitoring, swift responses to microseismic activities detected at the deployment sites, enabled by the utilization of advanced visualization tools.

The monitoring center further reinforces the decision support systems by promptly conveying alerts, automated report generation, and dispatch of notifications to researchers. In cases where genuine alerts are identified, immediate communication with disaster management authorities ensues, facilitating prompt necessary actions and interventions. This coordinated approach, substantially enhances the system's efficacy in vigilant monitoring of microseismic events in areas susceptible to landslides.

The data centers continuously monitor seismic activities in real-time, over extended periods, identifying any unusual or anomalous patterns that call for immediate attention. Leveraging the insights derived from regional-level analysis, can lead to improved assessment of future seismic events, based on historical data and ongoing monitoring efforts.

III. METHODS

This section discusses the experiments conducted in landslide laboratory test setups, outdoor deployments to validate the functionalities of the proposed microseismic sensing system in landslide-prone areas, and the data processing methods used for the characterization of the acquired microseismic signals.

A. LANDSLIDE LABORATORY TEST SETUPS

A laboratory setup, depicted in Figure 4, integrates advanced features for the scientific simulation of landslides. These features encompass variable slope angles, the ability to simulate diverse soil layer compositions reflecting field conditions, variability in rainfall rates, and dynamic pore pressures [12].

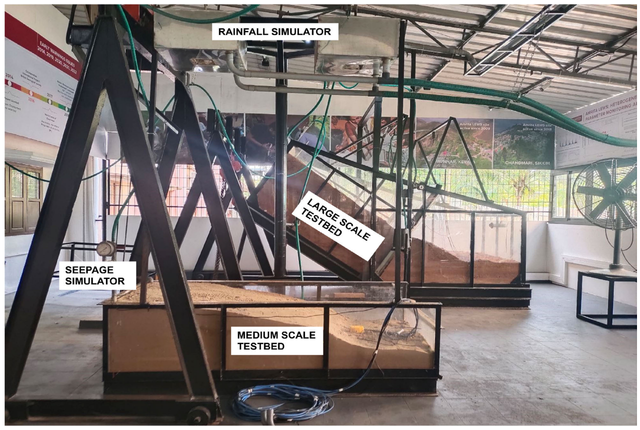

FIGURE 4. Set up of landslide testbeds.

The laboratory houses a medium-scale test bed of (1400 mm x 500 mm x 400 mm) dimensions capable of holding 2 tons of soil and a large-scale test bed of (1400 mm x 500 mm x 908765 mm) accommodating up to 8 tons of soil, facilitating realistic landslide simulations. Both the test beds incorporate a seepage simulator designed to replicate underground water movement with precise control over seepage rates and water pressures. The simulator can handle multiple seepages, at varying levels to simulate diverse flows across soil layers, alongside flow meters and pressure gauges integrated into the rainfall and seepage simulators for accurate measurement of flow rates.

The test beds are equipped with adjustable slope angles ranging from (zero to 45) degrees, enabling the simulation of varied geomorphic scenarios, supported by angle gauges for precise measurements. Additionally, the setups include rainfall simulators with a controlling valve to replicate varying intensities of rainfall. Specialized sprinklers attached (1)-(2) meters above the soil surface ensure even water distribution, accurately mimicking natural rainfall patterns.

Furthermore, the laboratory setup features a soil compactor for achieving different degrees of soil compaction, complemented by a compaction meter for quantification of compaction levels. The setups allow to simulate multiple depths of soil layers, facilitating homogeneous and stratified soil configurations. Testbeds can also incorporate vegetation effects for a more realistic simulation. The laboratory setup serves as a platform for calibration of geological sensors prior to their field-deployment in real-world scenarios.

B. EXPERIMENTATION IN LANDSLIDE LABORATORY

The experiments represent a critical validation phase of the proposed data acquisition system, apropos landslide early warning systems. The test plan was drawn to provide insights into responses from geophone sensors under laboratory-controlled conditions. This assessment showcases the proffered system's versatility in capturing simulated landslide

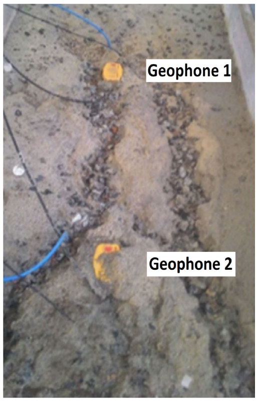

(a) Geophone signal Acquisition through Laboratory Simulations

(b) Outdoor trials for Vehicle and Pedestrian Geophone signal Acquisition

FIGURE 5. Experimentation for data collection.

events, attesting its readiness for general field deployment for early warning for landslides.

For conducting experiments, the medium-scale test bed was utilized, filled with a four-layer soil structure. The latter included clay, a mixture of gravel and boulders, a combination of sand and clay, and a mix of sand and rocks. The slope angle was precisely set to 35 degrees and maintained consistently throughout the experiment, mirroring a natural hill slope within the laboratory setting. Multiple geophones were installed onto the testbed, and the proffered sensing system was used to acquire geophone signals at 1 kHz, for each channel. The rainfall was simulated for a continuous duration of eight hours at a precipitation rate of 45 mm/hour. The rainfall contributed to saturation of the soil layers in the testbed. Incessant water infiltration increases the pore pressure, eventually leading to slope instabilities, as shown in Figure 5).

C. OUTDOOR FIELD TRIALS

Outdoor experiments were conducted in a road serving vehicle and pedestrian traffic, to simulate real-world conditions, as shown in Figure 5b). The signals associated with traffic movements were acquired by the proffered sensing system, to capture and understand the associate noise patterns. This included ten trials of single and multiple pedestrians engaged

FIGURE 6. Geophone sensor placement at the deployment site at chandmari, sikkim.

with different activities (jumping, walking, running, etc.) and capturing the movement of lightweight vehicles at a constant speed of around (20-25) km/hr.

D. REAL WORLD DEPLOYMENT

The real-time monitoring of microseismic signals, in landslide-prone mountainous regions, was achieved by deploying a network of the proposed SM-s nodes. This approach provided a comprehensive understanding of regional variability and facilitated better decision-making, during various triggering factors in landslide-prone regions.

1) STUDY REGION

The state of Sikkim, located in the northeastern part of India, encounters heightened risks within this geologically active and fragile Himalayan mountain range, rendering it fertile ground for the study of landslide dynamics and development of effective monitoring systems [9], [10], [11]. The region's geological complexity, exemplified by major thrust faults-Main Boundary Thrust (MBT) and the Main Central Thrust (MCT) and highly jointed rocks undergoing continuous deformation, presents arduous drilling activities, with exacerbated vulnerability to landslides and mass movements [23]. Chandmari, a locality in Gangtok, East Sikkim District, was identified as the study area due to its tracked history of numerous landslides during the monsoon season [49]. It is important to note that the region is classified as a high-risk seismic zone IV on the Indian seismic zoning map. The region encompassing the deployment site experienced moderate earthquakes, involving thrust motions and strike-slip motions, at the fault lines [10], [11], [14].

2) SENSOR PLACEMENT

This study utilized Deep Earth Probes (DEPs), an integrated monitoring module constituted of several heterogeneous sensors as part of the real-time Landslide Early Warning system [1]. Drilling for the placement of sensors is arduous due to the loose soil and fragile rocks in the site area. For

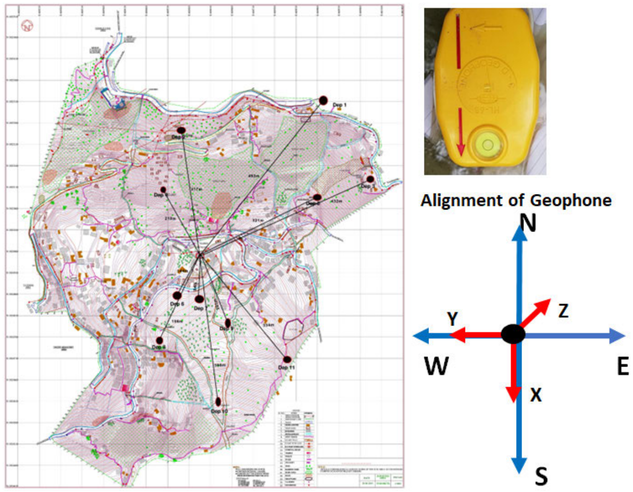

FIGURE 7. **Chandmari Geophone DEP Locations (black colored dots), and geophone alignment at each location. [49].**

the placement of sensors in the ground, small square wells were dug manually, to minimize inadvertent disturbance to the earth. Figure 6 shows the placement of geophones at one of the test site locations. The geophone spikes were fixed firmly, carefully oriented parallel to the ground, using built-in level indicators. Furthermore, the entire setup was made waterproof to protect geophones from rainfall or other precipitation. The sensor configuration was seamlessly integrated with the smart microseismic sensing system, transforming into a fully functional IoT edge node.

3) FIELD DEPLOYMENT OF SMART MICROSEISMIC SENSING SYSTEMS

Prototypes of the microseismic edge-based geophone sensing systems were strategically deployed at different positions, termed as DEP locations, in the hilly terrain, such as the toe, middle, and crown regions. The fully operational SM-s nodes, shown as black colored dots in Figure 7, provide crucial microseismic data for early warning systems and advancing research on landslides and seismic activity in the region. Its uninterrupted functionality ensures a reliable and valuable microseismic sensing system for large-scale spatiotemporal monitoring in landslide-prone regions.

A sample DEP location is shown in Figure 8. Since the time of its pilot deployment in 2018, the state-of-the-art geophone-based microseismic sensing systems have been effectively capturing and transmitting data to the FMC located in the landslide-prone region of Chandmari.

E. DATA PROCESSING METHODS

The SM-s nodes play a crucial role in capturing ground movements stimulated by various sources, encompassing surface and subsurface activities. However, these vibrational signals from geophones are susceptible to significant influences from environmental factors, fluctuations in temperature, power line interferences, and sensor drift. Examination of the study

FIGURE 8. **A DEP location where one of the SM-s Node is deployed at Chandmari, Sikkim.**

area, detailed in section III-D1, unveiled potential sources of signal interference- nearby water streams, shrubs and trees, roads, pedestrian pathways, wildlife, and construction activities. High-voltage transmission power lines nearby can introduce additional noise into the geophone signals. Given the diverse noise sources, comprehensive characterization of the microseismic signals was called for, to differentiate them from the surrounding noise sources at the deployment site. Signal processing techniques enabled the identification of noise patterns, their elimination, and the inference of relevant noise-minimized microseismic information from the geophone data [50].

A multi-tier signal processing frame work was utilized for characterizing the geophone signals. Firstly, the streaming values of voltage from geophones were extracted from the three channels, X, Y, and Z axes. The three-channel data formed the basis for subsequent processing. To eliminate any DC offset or baseline drift, mean normalization was applied. This step ensured that the data was centered around zero, which is essential for accurate signal analysis. A digital Butterworth LPF was utilized to improve signal quality. The filter parameters, and the filter order, were optimized for removal of high-frequency noise, to preserve the essential components of the acquired signal. The preprocessed geophone signals were also subjected to a series of bandpass filters. Each filter had a specific cutoff frequency range, such as (0-5) Hz, (5-10) Hz, (10-20) Hz, and so on. This step was undertaken to comprehend the frequency characteristics of the data within a particular range, which helps identification of dominant frequencies, frequency-spreads, and noise patterns that may be site-specific.

The geophone signals were put through a Short-Time Fourier Transform (STFT) analysis, to discern the frequency range of the acquired signal, providing valuable insights into the characteristics and dynamics of the microseismic activities [50], [51], [52]. Withal, the changes in ground motion parameters such as Peak Ground Acceleration (PGA), Peak Ground Velocity (PGV), and Peak Ground Displacement (PGD) were estimated using OpenSeismoMatlab [53], aiding in understanding the precursory activities associated with the slope instabilities under study.

IV. RESULTS AND DISCUSSIONS

This section presents findings derived from executing validation tests of the proposed microseismic sensing system in controlled laboratory settings and outdoor field trials. It further delves into the preliminary analysis of microseismic geophone signals, captured from real-world environments intricately linked with the causative factors of these natural disasters, all aimed at establishing effective early warning systems.

A. LABORATORY SIMULATIONS: SLIP SURFACE MOVEMENTS

The geophone signals captured during the landslide laboratory simulation represented slip surface movements, with signals from the crown (G1) and middle (G2) geophones shown in Figure 9. They depict the downslope movement of soil material along the slip surface of the testbed. The geophone signals from three channels are portrayed using a spectrogram to discern their attributes and track changes in frequency over time. Owing to the distinct sensor positions, there is a noticeable delay in data capture. The signal's evolution, as the soil descends the slope, is distinctly observable, with G1 at the crown registering the onset of the sliding movement, followed by a slight delay in data capture by G2 as it progresses downwards, as shown in Figure 9a) and 9b).

This behavior mirrors that of an actual landslide event, as evidenced by the spectrogram displaying high intensity in the middle, signifying the transmission of energy from the crown to the middle. The signals were acquired at the rate of 1 kHz, each spanning 1 minute 30 seconds and 1 minute 10 seconds. The signals showed maximum strength in the frequency range of (0-5) Hz at both positions. Besides, consistent frequency ranges between (10-20) Hz were observed, which could be attributed to interferences from the ambient environment. The analysis revealed frequencies below 5 Hz, consistent with the anticipated frequency range for landslide signals as reported in [36].

B. OUTDOOR FIELD TRIALS: PEDESTRIAN AND VEHICLE MOVEMENTS

Figure 10a) shows one of the trials for footstep movement, which lasted for a duration of 40 seconds. The accompanying spectrogram effectively captures the occurrence of footsteps at regular intervals, revealing a fundamental frequency range of (0.5-1) Hz. This periodicity indicates that the footstep signal repeats itself approximately every 1 to 2 seconds. As the individual approaches while walking, the strength of the footstep signal increases over a frequency range of (20-50) Hz. This behavior is expected, as the footstep signals are distinctly pronounced when the person is closer to the geophone. Conversely, as the individual moves away, the strength of the footstep signals decreases, resulting in a gradual decline in signal amplitude. However, the spectrogram also reveals the presence of consistent frequency interference around 10 Hz. These interfering frequencies are likely due to noises from the ambient environment.

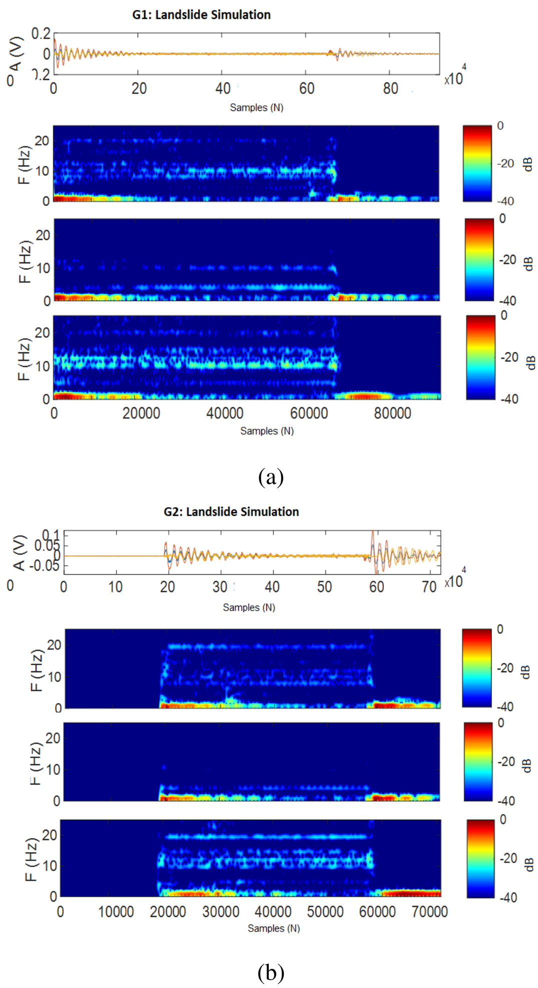

FIGURE 9. Recorded Signals of slip movements by the two geophone sensor systems a) G1 at crown b) G2 at middle region and their respective spectrogram for each channel.

One of the trials for vehicle movement is shown in Figure 10b) lasting 28 seconds, captured by the geophone sensor system. The accompanying spectrogram analysis effectively captures the vehicle movements, reaching frequencies of up to 60 Hz. Notably, the strength of the frequencies persists for (2.0-4.8) seconds, particularly as the vehicle approaches

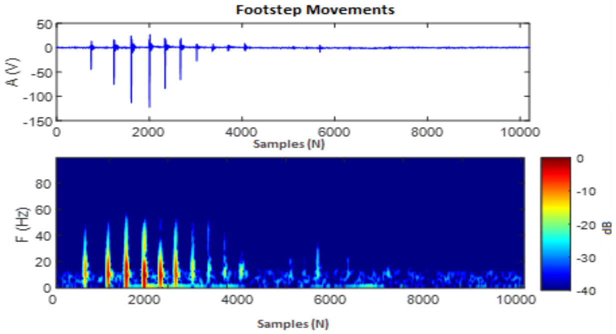

(a)

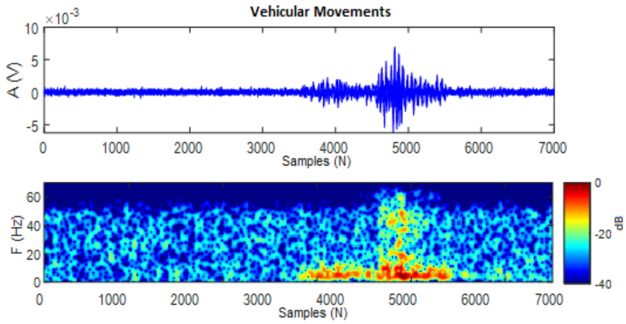

(b)

FIGURE 10. Recorded signals captured by a geophone sensor system for a) footstep and b) vehicular movements and their respective spectrogram.

closer to the geophones. This behavior is indicative of the vehicle's proximity to the sensor. Moreover, in the frequency spectrum, a prominent strength is observed around (10-15) Hz, which gradually increases up to the range of (50-60) Hz before decreasing again to around (10-15) Hz. These variations in frequency content can be attributed to specific vehicle engine sounds and their harmonics, which become more pronounced as the vehicle gets nearer and gradually recedes. The findings are consistent with the expected footstep monitoring and vehicular movement frequencies reported in [20].

Table 2 lists the observations from laboratory and outdoor experimentation. The results indicate that human and vehicular movements can generate vibrations and signals that overlap the frequency ranges of microseismic events, despite their distinct characteristics.

C. PRELIMINARY ANALYSIS OF MICROSEISMIC SIGNALS: DEPLOYMENT SITE, CHANDMARI

The slope instabilities, captured by the deployed SM-s nodes in Chandmari, correlated with earthquakes and rainfall precipitation events in the vicinity of the test site. Table 3 displays a few events recorded by the SM-s nodes, corresponding to the triggers for slope instability, type of movement, observed range of frequencies, and the estimates of ground motion. This highlights the proposed sensing system's effectiveness in capturing the microseismic precursor signals of the factors triggering landslides.

TABLE 2. Observations from lab and outdoor simulations.

Simulations	Type of movement	Duration (seconds)	Observed Range of Frequency
Landslide Lab	Slip Surface	(70-90)	(0- 5) Hz
Outdoor trials	Footsteps	(1.0-.02)	(20-50) Hz
Outdoor trials	Vehicles	(2.0-4.8)	up to 60 Hz

1) GEOPHONE SIGNAL RESPONSE FOR SLOPE INSTABILITIES DURING EARTHQUAKE TRIGGERS

As noted in Table 3, E1 refers to an earthquake, on September 12, 2018, measuring 5.5 on the Richter scale that struck the Kokrajhar District in Assam, India [54]. The quake occurred at approximately 10:20:49 AM Indian Standard Time (IST), with the epicenter at 26.4°N and 90.1°E. Despite being around 187 km away from the epicenter, the proposed system for geophones was able to record the microseismic triggers of this tremor event at three different DEP locations: DEP 8, DEP 10, and DEP 5.

Figure 11 shows the time domain representation of the geophone data captured by the monitoring system from the three DEP locations. For further analysis, the geophone signals were cropped to cover a total duration of approximately 1 hour, including half an hour both before, and after the time of the earthquake incident. Figure 11a), shows significant ground movements that persisted for about 2.4 minutes. Notably, the signal exhibited substantial strength within the frequency range of (0 -10) Hz, with dominant frequency peaks concentrated around (1-2) Hz.

In Figure 11b), notable changes in signal strength lasting for about 1.33 minutes can be observed. The dominant spectral range, (below 5 Hz) which was consistent throughout this event can be due to electrical interferences of that channel. It is observed that there is a dominant range of (0.5-1) Hz across all channels, around 1.33 minutes. In Figure 11c), the ground shakings due to the earthquake triggers caused a sudden drop in frequency ranges, with the effect lasting for approximately 15 minutes. However, higher frequencies up to 30 Hz were observed in the spectrum throughout this event, which can be due to electrical interferences of the channels itself.

Ground motion parameters, PGA, PGV, PGD, alongside the occurrence of earthquake triggers, were estimated for the 24 hour-geophone data from 9 to 25 September 2018. Figure 12) displays the fluctuations in ground motion parameters, where a significant increase followed by a gradual decrease in the values was observed during the event.

Earthquake event, E2, a 5.4 magnitude earthquake occured on March 20, 2020, approximately 153 km NW of Yuksom, Sikkim, India, at 07:03:17 IST. This event was followed by two more quakes on March 25, 2020, measuring 3.8 and 3.3 on the Richter scale; the first earthquake occurred at 05:09:32 IST, 167 km NNW of Yuksom, Sikkim and the second tremors were recorded at 04:43:25 IST, 197 km NW of Yuksom, Sikkim. [54]. The proposed microseismic system, situated approximately 40 km away from the epicenter at Yuksom, Sikkim captured the slope instabilities, as shown

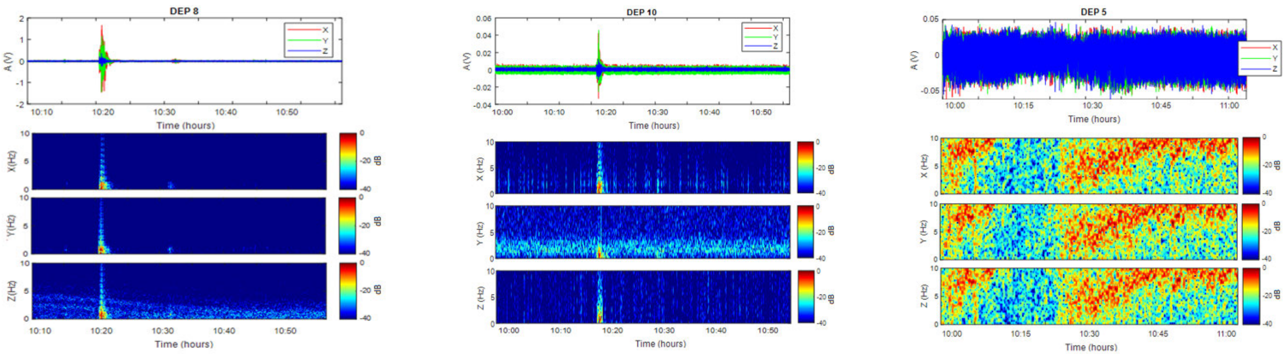

(a) DEP 8 (b) DEP 10 (c) DEP 5

FIGURE 11. Geophone Signals captured by the developed microseismic system at three DEP locations at the deployment site, Chandmari during the slope instability caused due to earthquake trigger recorded on 12 September 2018.

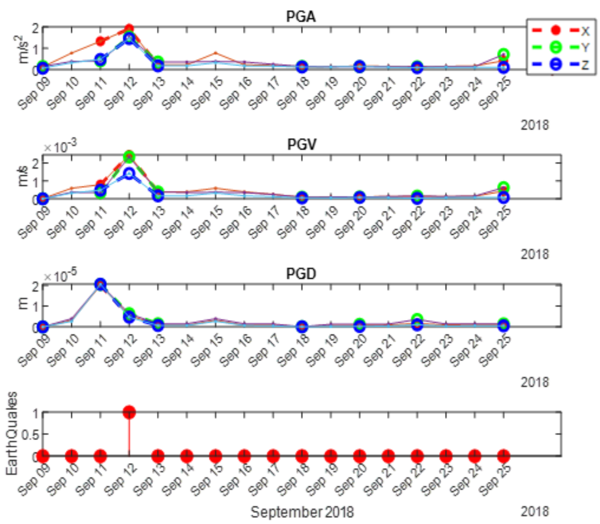

FIGURE 12. Variation of the Ground Motion Parameters: Peak Ground Acceleration (PGA), Peak Ground Velocity (PGV), Peak Ground Displacement (PGD), and occurrence of slope instability due to earthquake trigger during September 2018, from DEP 9.

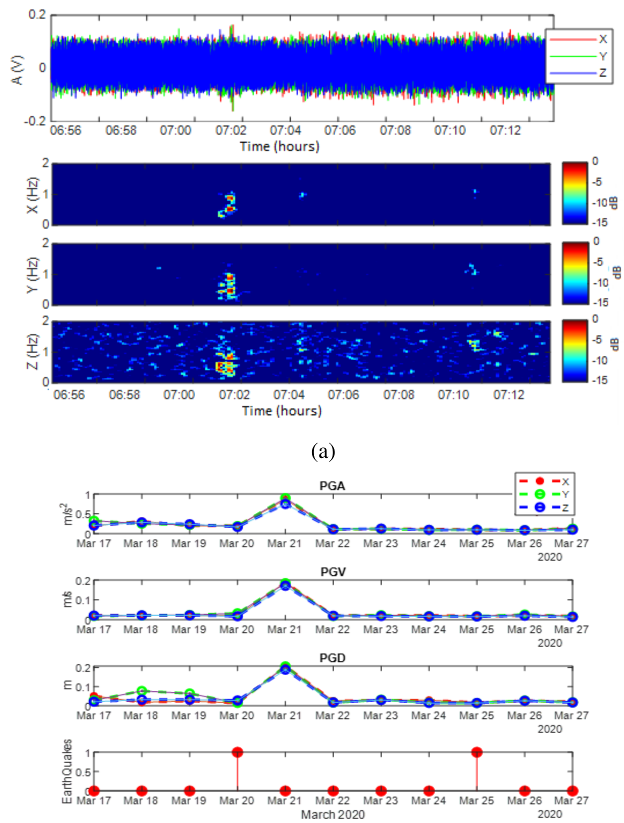

(a)

(b)

FIGURE 13. a) Geophone Signals captured by the developed microseismic system during slope stability due to earthquake trigger recorded on 20 March 2020 b) Variation of the Ground Motion Parameters: PGA, PGV, PGD, and occurrence of slope instability due to earthquake triggers during March 2020, from DEP 9.

in Figure 13. The spectrogram revealed a prominent range of (0.1-1.0) Hz, lasting less than 3 minutes. Other consistent frequencies observed in the spectrum can be due to the electrical interference in the channel.

Figure 13b) reveals a gradual increase in ground motion parameters after the earthquake event on March 20, 2020, indicative of the aftershocks in the region. However, for the events on March 25, feasible variations in ground motion parameters were evident. The results shown in Figure 12 and Figure 13b) provide valuable insights into ground motion variations associated with ground shakings in the region subsequent to the earthquake events. The significant decrease in ground motion parameters observed during and after the tremor events suggests that these variations could serve as precursors for the detection of slope instabilities set in by ground shaking. However, arriving at conclusive findings mandate a thorough analysis, which is beyond the scope of this paper's investigation.

2) GEOPHONE SIGNAL RESPONSE FOR SLOPE INSTABILITIES DURING RAINFALL TRIGGERS

Figure 14 shows the available rainfall data collected from the Indian Meteorological Department for the district of East Sikkim for the years 2018-2021 [55]. It reveals that heavy rainfall was experiences during the period from April to

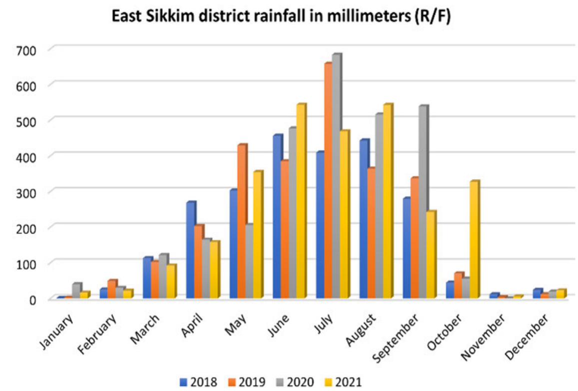

FIGURE 14. east sikkim rainfall data for the years 2018-2021.

FIGURE 15. Slope instabilities near the site, triggered by rainfall.

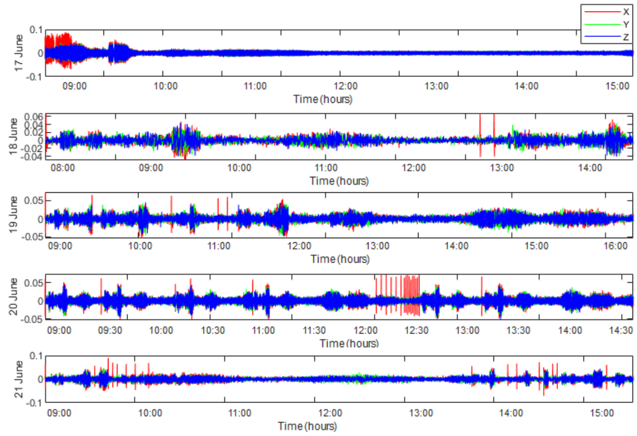

(a)

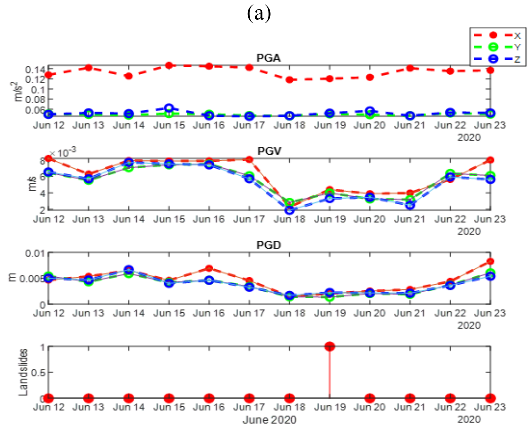

(b)

FIGURE 16. a) Time domain representation of the slope instabilities observed in the geophone data during the period 17-21 June 2020 for the corresponding event observed on 19 June 2020, b) Variation of the ground motion parameters during the period June 12-23, 2020, from DEP 9.

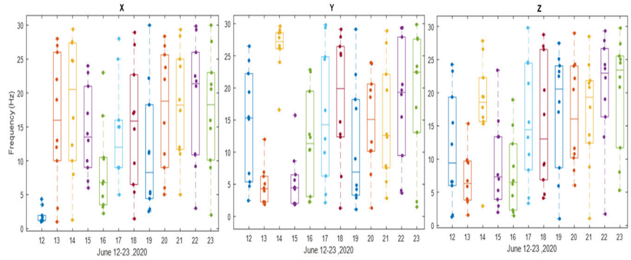

FIGURE 17. Variations observed in dominant frequency ranges at each channels, during the period June 12-23, 2020, from DEP 9.

September. A comparison of the cumulative rainfall for June and July shows an increase in the downpour from 432.45 mm in 2018 to 579.85 mm in 2020 and 542.7 mm in 2021, highlighting the increased probability of landslides at the selected field site during the rainy season.

The slope instability caused by the sliding movement of rock-debris, referred to as E3, was triggered following heavy rainfall, on 19 June 2020, around 450 meters away from one of our site locations at 27°20.371‘‘N 88°37.552’’E, as shown in Figure 15. The geophone signals were recorded during the slope instabilities, due to rainfall triggers that happened in the days as depicted in Figure 16a). The variation of the ground motion parameters during the period (12-23) June 2020, from the location DEP 9 is shown in Figure 16b). It depicts that there was an increase in the amplitude of the ground motion parameters (3-4) days before the recorded event and a significant decrease a day before the event. These variations could serve as precursors for detecting slope instabilities of landslide initiation and seismic events.

Figure 17 shows the variations in dominant frequency ranges, which may be due to rainfall and external noises generated by the rain over time. This suggests that the impact of the heavy rainfall on the frequency range was initially more severe, with sudden increase and decrease, which stabilized in the following days, to the typical range of (15- 28) Hz, which is considered as the frequency ranges observed during normal day scenarios.

Table 3 shows the observed dominant frequency ranges of the geophone signals, correlated with triggers for the recorded events at the Chandmari deployment site. The frequency ranges differ depending on the specific site conditions, and the underlying geology. Nevertheless, this indication could serve as supplementary information, when combined with data from other sensors [13], [56], [57]. Doing so, enhances

TABLE 3. Observations from geophone signals from chandmari.

Events	Triggers for slope instability	Location	Type of movement	Dominant Frequency Range
E1	Earthquake	DEP 8	Ground Shaking	0-10 Hz
		DEP 10		(0-5) Hz
		DEP 5		(up to 30) Hz
E2	Earthquake	DEP 9	Ground Shaking	(<5) Hz
E3	Rainfall	DEP 9	Rock/Debris Slide	(up to 30) Hz

the efficacy of decision-making support systems, with a clear link established between frequency ranges and signs of slope instability during the rainy season. This necessitates further exploration of the geophone signals during specific weather conditions, which suggest ongoing creep and subsidence movements, indicative of impending landslides.

Findings from laboratory experiments and field deployments highlight the potential of the proposed microseismic sensing system to capture earth tremors, even the subtlest microseismic triggers. This establishes the foundation for a cost-effective, non-intrusive, and long-term spatiotemporal monitoring solution, laying the groundwork for an efficient early warning system in landslide-prone areas. The results of the analysis from the geophone-based sensing systems can be cross-referenced with other sensor data to enhance early warning capabilities. However, achieving accurate event detection mandates a precise distinction between relevant signals and background noise, which compel focused effort on refinement of signal processing algorithms, and its applicability at the edge. Enhancement of context-aware data and energy management techniques can significantly conserve power consumption in edge sensing systems, thereby extending system lifetime and effective manipulation of resource constraints [40], [58].

D. LIMITATIONS

Albeit the proposed microseismic sensing system affords promising capabilities for landslide detection and early warning, careful consideration of potential risks and challenges is imperative to maximize its effectiveness, and minimize adverse impacts. One of the significant risks is the likelihood of false alarms or misinterpretation of micro-seismic signals, leading to unnecessary panic. The proposed solution has taken into account scenarios such as misinterpretation of microseismic signals due to footsteps, and vehicular movements. The solution includes methodologies to detect and classify these signals, thereby avoiding false alarms. In addition, misinterpretation of signals during initiation of slope instability has been mitigated by integrating heterogeneous sensors, capable of monitoring multiple trigger types that are prominent in different stages of the slope instability initiation pathway [12], [49], [56].

It is also important to consider events such as the gradual movement of slopes by creep landslides, causing sensor malfunction and the possibility of power loss due to extreme weather conditions in remote or rugged terrain, such as the Himalayas. Although context-aware energy management systems have been implemented [40], extreme weather conditions may still result in power loss, preventing the system from operating or leading to data loss during transmission. Logistical and operational challenges may turn up when installing the system in remote or rugged terrain. These include maintainence and calibration of the sensor network, to ensure data integrity and security, and managing power sources in off-grid locations. Attention to these potential hurdles is crucial for ensuring the long-term viability of the proposed system.

V. COMPARISON WITH EXISTING SYSTEM

An assessment was conducted to evaluate whether the presented research adequately addressed key functionalities denoted as F1-F11, derived from the requirements discussed in section I. Table 4 presents a curated selection of publicly available research focused on microseismic monitoring using in-situ geophysical methods, to detect triggers that ensue in landslides. The existing microseismic studies primarily address single triggers with limited data rates and lack real-time and early warning capabilities, which renders them ill-suited for spatio-temporal monitoring. As a result, achieving a fair comparison with previous approaches is not feasible. Nevertheless, the study aims to present some comparative analysis. Table 4 outlines the applications and sensing instruments utilized in the literature.

- F1: High frequency data capture-Incessant acquisition of data samples.
- F2: Microseismic data acquisition- Generation of seismic waves from ground/ anthropogenic activities/ industrial processes.
- F3: Resource constraints- Limited processing, storage potential, minimum power in IoT environment.
- F4: Continuous, and real time monitoring- Delivery of continuous microseismic data
- F5: Large scale spatio-temporal monitoring- Extensive surveillance and perusal of a vast geographical area over an extended period.
- F6: Precursor signal detection- Identify early pre-triggers associated with F2.
- F7: Microseismic activity detection- Methods for detecting microseismic data, related to F2.
- F8: Early warning capabilities
- F9: Mapping to microseismic triggers- due to heavy rainfall, seismic activity.
- F10: Communication Technology- Data transmission or local storage.
- F11: Monitoring Period- Short term (Monthly, or shorter durations), Long term (Yearly or longer durations)

A critical review of 20 selected articles in the field of microseismic monitoring was conducted to compare them with the proposed system. Figure 18 presents the

TABLE 4. Comparison of existing systems and proposed system.

Year [Ref.]	Applications	Sensing Instruments	F1	F2	F3	F4	F5	F6	F7	F8	F9	F10	F11
2012, [59]	Debris flows, moving boulders	Geophones	Yes	Yes	No	No	No	No	Yes	Yes	No	*Nil	Short term
2012, [60]	Rockfalls	Geophones, ultrasonic devices, Cameras	Yes	Yes	No	No	No	No	Yes	Yes	No	*Nil	Short term
2017, [61]	Earthquakes, Ground motions	Smartphone MEMS, GPS	No	Yes	No	Yes	Yes	No	Yes	Yes	No	Wi-Fi, 2G/3G /4G	Long term
2017, [62]	Deep seated landslides, debris, cracks and rock slides	PWP , accelerometers, soil moisture sensor, rain gauge	No	Yes	No	Yes	Yes	No	Yes	Yes	Yes	Zigbee, GSM/ GPRS	Short term
2018, [63]	Earthquakes, Ground motions	Geophones	No	Yes	No	No	Yes	Yes	Yes	Yes	No	Ethernet	Short term
2019, [64]	Structural health monitoring	Inclinometers	No	No	No	Yes	Yes	No	Yes	Yes	No	CANopen	Short term
2019, [65]	Earthquakes, Ground motions	MEMS accelerometers	No	Yes	No	Yes	No	No	Yes	Yes	No	Ethernet, 3G/4G	Short term
2019, [66]	Earthquakes, Ground motions	MEMS accelerometers	No	Yes	No	Yes	No	No	Yes	Yes	No	3G/4G	Long term
2019, [67]	Structural health monitoring, Earthquakes, Ground motions	Optic fiber, MEMS and piezoelectric sensors	No	Yes	No	No	Yes	No	Yes	Yes	No	MBUS radio 169 MHz, 5G	Long term
2019, [68]	Gravity-driven failures, steep active rock glacier	Geophones	Yes	Yes	No	No	No	Yes	Yes	Yes	Yes	*Nil	Long term
2020, [69]	Earthquake, infrastructure failures	GPS Stations, seismometers	Yes	Yes	No	No	No	No	Yes	Yes	Yes	*Nil	Short term
2020, [70]	Earthquakes, Ground motions	Seismometers	Yes	Yes	No	Yes	No	No	Yes	No	No	*Nil	Short term
2020, [71]	Earthquake	Smartphone MEMS	No	Yes	Yes	Yes	Yes	Yes	Yes	Yes	Yes	Wi-Fi, 3G/4G	Long term
2020, [56]	Deep seated landslides, surface soil investigation, slow ground monitoring	Rainfall, pore water pressure sensors	No	No	No	Yes	Yes	No	No	Yes	No	3G/4G, LoRa	Long term
2020, [72]	Landslide, debris flow, rockfall	Weather and ground nodes	No	Yes	Yes	No	Yes	No	Yes	No	No	LoRa	Long term
2021, [73]	Shallow rotational landslides	Continuous Shear Monitor, piezometers extensometer, inclination and water sensor	No	No	Yes	Yes	Yes	No	No	Yes	No	LoRa, GSM	Long term
2021, [74]	Creeping slopes, ground motions	GNSS station; ground crack, rainfall monitoring station	No	Yes	Yes	No	Yes	No	Yes	Yes	Yes	5G, GPRS	Long term
2021, [75]	Oil and gas exploration, land seismic acquisition	Geophones	Yes	Yes	No	Yes	Yes	No	Yes	No	No	IEEE 802.11	Short term
2022, [76]	Rock slides, rock cracks	Geophones, accelerometers	Yes	Yes	No	Yes	No	No	Yes	No	Yes	4G, Wi-Fi	Short term
2022, [77]	Landslide dam breaching	Broadband seismometers, geophones	No	Yes	No	No	No	No	Yes	Yes	Yes	*Nil	Short term
Proposed System	Landslides, Earthquakes, Ground motions	Geophones	Yes	Yes	Yes	Yes	Yes	Yes	Yes	Yes	Yes	Wi-Fi	Long Term

*Nil: Not mentioned.

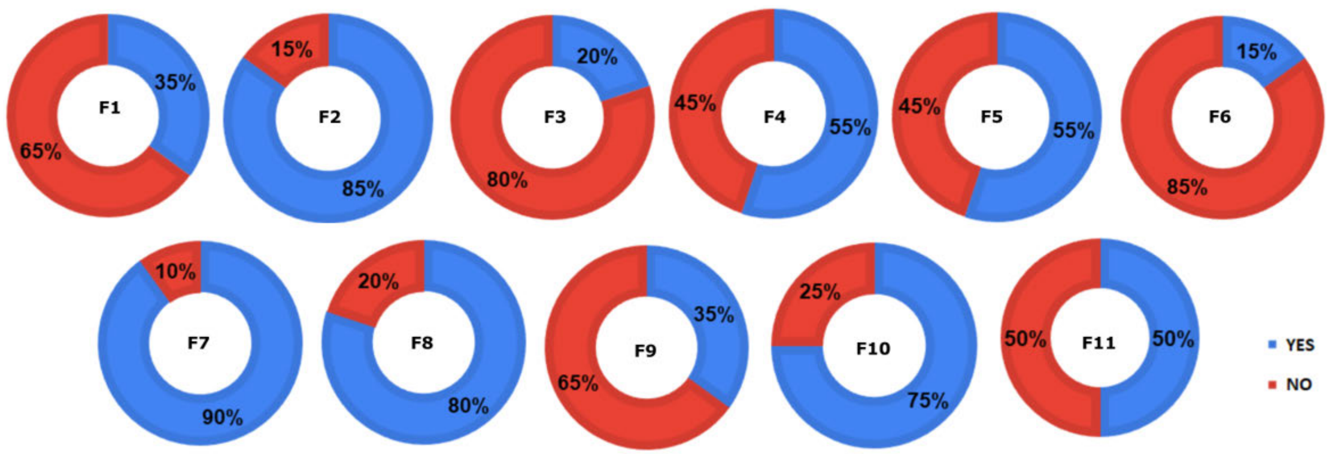

FIGURE 18. Comparative analysis with the exisiting systems.

comparative analysis of these reviewed articles, highlighting factors F1 through F11. Firstly, 85 % of the reviewed studies emphasize the importance of capturing microseismic data (F2), and 90 % discuss methods for microseismic activity detection (F7). Additionally, 80 % consider their applications to have early warning capabilities (F8), and 75 % use standard communication technologies for data transmission (F10), the remaining 25 % either do not specify their methods or rely on local storage. However, only 35 % focus on high-frequency data capture (F1), revealing an underutilization of high-frequency microseismic signals that could provide more detailed insights into landslide dynamics.

Furthermore, 20 % of the reviewed studies consider resource constraints in the development of IoT systems (F3), highlighting the need for further research into cost-effective and efficient IoT solutions for resource-limited regions. Only 15 % of the investigations explore precursory triggers and the detection of landslides (F6), indicating a pressing need for more research into identifying and understanding early warning signs. Additionally, 35 % of the studies fail to adequately map microseismic triggers (F9), suggesting a gap in integrating microseismic data with geological and environmental factors. 50 % of the reviewed studies focus on short-term monitoring, which can be monthly or even shorter, while the other 50 % focus on long-term monitoring, considered as yearly or more. Moreover, 45 % of the studies lack systems capable of large-scale spatiotemporal and real-time monitoring (F4, F5), underscoring a significant paucity in comprehensive monitoring capabilities. This comparative analysis emphasizes the critical areas where advancements are needed, particularly in high-frequency data capture, integration of microseismic data with environmental factors, comprehensive monitoring capabilities, and cost-effective IoT solutions.

A few studies satisfiying the minimum functionalities are detailed below. The study in [74] discusses an IoT based landslide monitoring and early warning system, offering accurate data acquisition of morphological change and disintegration pattern of the landslide body, fast transmission, and comprehensive analysis in creep slopes on a continuous basis. However, such systems have limitations, including lower data transmission rates, lack of microseismic signal capturing, and spatiotemporal monitoring capabilities. Studies such as [61] and [78] presents insights into technologies for landslide monitoring, while [62], [68] discuss the design and experimental systems for detecting early signs of landslide events using integrated sensors but lack a comprehensive framework and end-to-end real-time system architecture.

Another study by [71], investigates early warning system frameworks for rapidly detecting earthquake ground motions, does not involve sensing hardware deployment or maintenance, but utilizes smartphones incurring high operational costs. Similar methodologies for landslide early warning systems with advanced capabilities remain limited. The existing systems in Table 4 cover only a portion of the essential functionalities required for effective microseismic monitoring, suggesting the need for a more comprehensive approach.

The proposed system, in comparison, showcases robust capabilities of the sensing system with its cost-effective passive sensing system, utilizing geophone sensors in detecting and monitoring microseismic events and their triggers. It captures microseismic vibrations at exceptionally high data rates (1 kHz, across each sensor channel), from multiple locations, fulfilling all functionalities, and provides numerous advantages over traditional monitoring methods [16], [19], [20], [21], [22]. The proposed system has been deployed in real-world scenarios supporting long-term large-scale spatio-temporal monitoring, and enabling the mapping of microseismic triggers associated with slope instabilities due to rainfall and earthquakes. The seamless connectivity of the proposed system significantly enhances its capability to deliver actionable insights to stakeholders, emergency responders, local authorities, and residents, marking a significant advancement in microseismic monitoring and early warning systems.

VI. CONCLUSION AND FUTURE DIRECTIONS

This paper presented an IoT-driven platform for the capture of subterranean microseismic vibrations in regions prone to landslides. The proposed microseismic edge sensing system, incorporating geophone sensors (SM-s nodes), was deployed to continuously record and transmit real-time microseismic data from landslide-prone areas of Chandmari, in the state of Sikkim, in North eastern Himalayas. The proposed system successfully captured the slope instability events in June 2020, and earthquake events in September 2018, and March 2020. Results from laboratory experiments and field deployments demonstrate the effectiveness of the proposed sensing system in capturing subtle pre-triggers of slope instabilities, precipitated by rainfall and earthquakes. This forms the basis for a cost-effective, non-intrusive, and long-term spatiotemporal monitoring solution, setting a robust foundation for an efficient early warning system in landslide-prone regions.

The proposed microseismic geophone sensing system demonstrated promising capabilities in monitoring a diverse range of geological phenomena such as rock falls, rock-slides, debris flows, earthquakes, snow avalanches, and other seismic activities induced by anthropogenic actions. The microseismic signal analysis will aid in understanding the principal mechanisms governing each stage of these potential hazards. It is crucial for the refinement of robust signal processing algorithms and comprehensive validation protocols, including real-time validation. Ongoing research involves analysis of microseismic data from various locations and cross-referencing with environmental factors, intended to be incorporated in future studies. The proposed system can be further enhanced to derive adaptive thresholds using detailed data analysis and machine learning approaches. This will contribute to real-time identification and classification of the characteristics and rate of landslide movements in different materials, enabling automatic classification and mapping of imminent landslides.

ACKNOWLEDGMENT

The authors express our deep gratitude to Sri Mata Amritanandamayi Devi (AMMA), Chancellor, Amrita Vishwa Vidyapeetham, who bestowed the motivation and inspiration to pursue this research work. They undertook this work following their recognition as the "World Center of Excellence in landslide disaster risk reduction," conferred on them by the "International Programme on Landslides," in August 2017, November 2021, and November 2023. They gratefully appreciate the contributions of the Entire Landslide Team in their research center for their support in various aspects. They acknowledge the valuable suggestions from Dr. Venkat Rangan, Prof. Balaji Hariharan, Dr. T. Hemalatha, Dr. M. Ravisankar, and Nitin Kumar. They wish to acknowledge the support provided by Sravan Thampan, Dawa Tshering Lepcha, Ramesh Guntha, Balmukund Singh, Dr. Rekha Prabha, Deepak Brahmanandan, and Arun Kumar Jijilal.

REFERENCES

[1] M. V. Ramesh, "Design, development, and deployment of a wireless sensor network for detection of landslides," *Ad Hoc Netw.*, vol. 13, pp. 2–18, Feb. 2014.

[2] A. Novellino, C. Pennington, K. Leeming, S. Taylor, I. G. Alvarez, E. McAllister, C. Arnhardt, and A. Winson, "Mapping landslides from space: A review," *Landslides*, vol. 21, no. 5, pp. 1041–1052, May 2024.

[3] *Public EM-DAT Platform*. Accessed: May 5, 2024. [Online]. Available: https://public.emdat.be

[4] M. J. Froude and D. N. Petley, "Global fatal landslide occurrence from 2004 to 2016," *Natural Hazards Earth Syst. Sci.*, vol. 18, no. 8, pp. 2161–2181, Aug. 2018.

[5] C.-W. Lin, S.-H. Liu, S.-Y. Lee, and C.-C. Liu, "Impacts of the chi-chi earthquake on subsequent rainfall-induced landslides in central Taiwan," *Eng. Geol.*, vol. 86, nos. 2–3, pp. 87–101, Aug. 2006.

[6] D. K. Keefer, J. Wartman, C. N. Ochoa, A. Rodriguez-Marek, and G. F. Wieczorek, "Landslides caused by the 7.6 Tecomán, Mexico earthquake of Jan. 21, 2003," *Eng. Geol.*, vol. 86, nos. 2–3, pp. 183–197, 2003.

[7] Z.-Y. Feng, C.-M. Hsu, and S.-H. Chen, "Discussion on the characteristics of seismic signals due to riverbank landslides from laboratory tests," *Water*, vol. 12, no. 1, p. 83, Dec. 2019.

[8] S. Cuomo, "Modelling of flowslides and debris avalanches in natural and engineered slopes: A review," *Geoenvironmental Disasters*, vol. 7, no. 1, pp. 1–25, Dec. 2020.

[9] R. Bhasin, E. Grimstad, J. O. Larsen, A. K. Dhawan, R. Singh, S. K. Verma, and K. Venkatachalam, "Landslide hazards and mitigation measures at Gangtok, Sikkim Himalaya," *Eng. Geol.*, vol. 64, no. 4, pp. 351–368, Jun. 2002.

[10] N. Vasudevan and K. Ramanathan, "Geological factors contributing to landslides: Case studies of a few landslides in different regions of India," *Proc. IOP Conf. Series, Earth Environ. Sci.*, vol. 30, pp. 011–012, Aug. 2016.

[11] N. Vasudevan, K. Ramanathan, and M. S. Ananthapathmanabhan, "Visual representation of slope stability for landslide monitoring systems," in *Proc. 4th Int. Conf. Converg. Technol. (I2CT)*, Oct. 2018, pp. 1–5.

[12] T. Hemalatha, M. V. Ramesh, and V. P. Rangan, "Effective and accelerated forewarning of landslides using wireless sensor networks and machine learning," *IEEE Sensors J.*, vol. 19, no. 21, pp. 9964–9975, Nov. 2019.

[13] M. V. Ramesh, D. Pullarkatt, T. H. Geethu, and P. V. Rangan, "Wireless sensor networks for early warning of landslides: Experiences from a decade long deployment," in *Proc. Workshop World Landslide Forum*, 2017, pp. 41–50.

[14] M. V. Ramesh and N. Vasudevan, "The deployment of deep-Earth sensor probes for landslide detection," *Landslides*, vol. 9, no. 4, pp. 457–474, Dec. 2012.

[15] H. Thirugnanam, S. Uhlemann, R. Reghunadh, M. V. Ramesh, and V. P. Rangan, "Review of landslide monitoring techniques with IoT integration opportunities," *IEEE J. Sel. Topics Appl. Earth Observ. Remote Sens.*, vol. 15, pp. 5317–5338, 2022.

[16] S. Uhlemann, A. Smith, J. Chambers, N. Dixon, T. Dijkstra, E. Haslam, P. Meldrum, A. Merritt, D. Gunn, and J. Mackay, "Assessment of ground-based monitoring techniques applied to landslide investigations," *Geomorphology*, vol. 253, pp. 438–451, Jan. 2016.

[17] T. Carla, T. Nolesini, L. Solari, C. Rivolta, L. Dei Cas, and N. Casagli, "Rockfall forecasting and risk management along a major transportation corridor in the Alps through ground-based radar interferometry," *Landslides*, vol. 16, no. 8, pp. 1425–1435, Aug. 2019.

[18] J. S. Whiteley, J. E. Chambers, S. Uhlemann, P. B. Wilkinson, and J. M. Kendall, "Geophysical monitoring of moisture-induced landslides: A review," *Rev. Geophys.*, vol. 57, no. 1, pp. 106–145, Mar. 2019.

[19] S. Pirasteh and J. Li, "Landslides investigations from geoinformatics perspective: Quality, challenges, and recommendations," *Geomatics, Natural Hazards Risk*, vol. 8, no. 2, pp. 448–465, Dec. 2017.

[20] V. N. Deekshit, M. V. Ramesh, P. K. Indukala, and G. J. Nair, "Smart geophone sensor network for effective detection of landslide induced geophone signals," in *Proc. Int. Conf. Commun. Signal Process. (ICCSP)*, Apr. 2016, pp. 1565–1569.

[21] V. Del Gaudio, J. Wasowski, and S. Muscillo, "New developments in ambient noise analysis to characterise the seismic response of landslide-prone slopes," *Natural Hazards Earth Syst. Sci.*, vol. 13, no. 8, pp. 2075–2087, Aug. 2013.

[22] A. T. Kunnath and M. V. Ramesh, "Integrating geophone network to real-time wireless sensor network system for landslide detection," in *Proc. 1st Int. Conf. Sensor Device Technol. Appl.*, Jul. 2010, pp. 167–171.

[23] D. M. Cruden and D. J. Varnes, "Landslides: Investigation and mitigation. chapter 3-landslide types and processes," *Transp. Res. board special Rep.*, vol. 247, no. 1, pp. 1–20, 1996.

[24] F. G. Murillo-García, M. Rossi, F. Ardizzone, F. Fiorucci, and I. Alcántara-Ayala, "Hazard and population vulnerability analysis: A step towards landslide risk assessment," *J. Mountain Sci.*, vol. 14, no. 7, pp. 1241–1261, Jul. 2017.

[25] P. Lacroix, A. L. Handwerger, and G. Bièvre, "Life and death of slow-moving landslides," *Nature Rev. Earth Environ.*, vol. 1, no. 8, pp. 404–419, Jul. 2020.

[26] T. R. Martha, N. Kerle, V. Jetten, C. J. van Westen, and K. V. Kumar, "Characterising spectral, spatial and morphometric properties of landslides for semi-automatic detection using object-oriented methods," *Geomorphology*, vol. 116, nos. 1–2, pp. 24–36, Mar. 2010.

[27] N. Hovius and P. Meunier, *Earthquake Ground Motion and Patterns of Seismically Induced Landsliding*. Cambridge, U.K.: Cambridge Univ. Press, 2012, pp. 24–36.

[28] D. M. Cruden and R. Couture, "More comprehensive characterization of landslides: Review and additions," in *Proc. 11th Int. IAEG Congr., Geologically Act.*, 2010, pp. 5–10.

[29] J. J. Clague and D. Stead, *Landslides: Types, Mechanisms Model*. Cambridge, U.K.: Cambridge Univ. Press, 2012.

[30] B. P. Bhandari and S. Dhakal, "A multidisciplinary approach of landslide characterization: A case of the siwalik zone of Nepal Himalaya," *J. Asian Earth Sci., X*, vol. 5, Jun. 2021, Art. no. 100061.

[31] N. Tisato and C. Madonna, "Attenuation at low seismic frequencies in partially saturated rocks: Measurements and description of a new apparatus," *J. Appl. Geophys.*, vol. 86, pp. 44–53, Nov. 2012.

[32] G. Koç and K. Yegin, "Footstep and vehicle detection using slow and quick adaptive thresholds algorithm," *Int. J. Distrib. Sensor Netw.*, vol. 9, no. 10, Oct. 2013, Art. no. 783604.

[33] A. E. Faghfouri and M. B. Frish, "Robust discrimination of human footsteps using seismic signals," *Proc. SPIE*, vol. 8046, May 2011, Art. no. 80460D.

[34] P. Anghelescu, G. V. Iana, and I. Tramandan, "Human footstep detection using seismic sensors," in *Proc. 7th Int. Conf. Electron., Comput. Artif. Intell. (ECAI)*, Jun. 2015, pp. 1–15.

[35] L. Yang, Y. Xu, L. Wang, and Q. Jiang, "Seismic signal characteristics and numerical modeling analysis of the Xinmo landslide," *Sustainability*, vol. 15, no. 7, p. 5851, Mar. 2023.

[36] Y. Yan, Y. Cui, X. Tian, S. Hu, J. Guo, Z. Wang, S. Yin, and L. Liao, "Seismic signal recognition and interpretation of the 2019 '7.2' shuicheng landslide by seismogram stations," *Landslides*, vol. 17, no. 5, pp. 1191–1206, May 2020.

[37] E. Por, M. van Kooten, and V. Sarkovic, "Nyquist–Shannon sampling theorem," *Leiden Univ.*, vol. 1, no. 1, p. 5, 2019.

[38] S. M. Karunarathne, M. Dray, L. Popov, M. Butler, C. Pennington, and C. M. Angelopoulos, "A technological framework for data-driven IoT systems: Application on landslide monitoring," *Comput. Commun.*, vol. 154, pp. 298–312, Mar. 2020.

[39] P. Maxwell and M. Lansley, "What receivers will we use for low frequencies?" in *SEG Technical Program Expanded Abstracts*. Houston, TX, USA: Society of Exploration Geophysicists, 2011, pp. 72–76.

[40] R. Prabha, M. V. Ramesh, V. P. Rangan, P. V. Ushakumari, and T. Hemalatha, "Energy efficient data acquisition techniques using context aware sensing for landslide monitoring systems," *IEEE Sensors J.*, vol. 17, no. 18, pp. 6006–6018, Sep. 2017.

[41] S. Kumar and M. V. Ramesh, "Lightweight management framework (IMF) for a heterogeneous wireless network for landslide detection," in *Proc. Int. Conf. Web Semantic Technol.*, 2010, pp. 457–471.

[42] R. Guntha, S. Kumar, and B. Hariharan, "Scalable, secure, fail safe, and high performance architecture for storage, analysis, and alerts in a multi-site landslide monitoring system," in *Advancing Culture of Living With Landslides*. Cham, Switzerland: Springer, 2017, pp. 61–69.

[43] D. Anikiev, C. Birnie, U. B. Waheed, T. Alkhalifah, C. Gu, D. J. Verschuur, and L. Eisner, "Machine learning in microseismic monitoring," *Earth-Science Rev.*, vol. 239, Apr. 2023, Art. no. 104371.

[44] Y. Pu, D. B. Apel, and R. Hall, "Using machine learning approach for microseismic events recognition in underground excavations: Comparison of ten frequently-used models," *Eng. Geol.*, vol. 268, Apr. 2020, Art. no. 105519.

[45] S. Kim, B. Yoon, J.-T. Lim, and M. Kim, "Data-driven signal–noise classification for microseismic data using machine learning," *Energies*, vol. 14, no. 5, p. 1499, Mar. 2021.

[46] W. Jinqiang, P. Basnet, and S. Mahtab, "Review of machine learning and deep learning application in mine microseismic event classification," *Mining Mineral Deposits*, vol. 15, no. 1, pp. 19–26, 2021.

[47] M. Shafiq, Z. Tian, Y. Sun, X. Du, and M. Guizani, "Selection of effective machine learning algorithm and bot-IoT attacks traffic identification for Internet of Things in smart city," *Future Gener. Comput. Syst.*, vol. 107, pp. 433–442, Jun. 2020.

[48] M. Shafiq, Z. Tian, A. K. Bashir, A. Jolfaei, and X. Yu, "Data mining and machine learning methods for sustainable smart cities traffic classification: A survey," *Sustain. Cities Soc.*, vol. 60, Sep. 2020, Art. no. 102177.

[49] G. T. Harilal, D. Madhu, M. V. Ramesh, and D. Pullarkatt, "Towards establishing rainfall thresholds for a real-time landslide early warning system in Sikkim, India," *Landslides*, vol. 16, no. 12, pp. 2395–2408, Dec. 2019.

[50] K. P. Soman, S. S. Kumar, N. Mohan, and P. Poornachandran, "Modern methods for signal analysis and its applications," *Recent Adv. Comput. Intell.*, vol. 1, pp. 263–290, Jun. 2019.

[51] U. V. Krishna, R. Priyamvada, G. Jyothish, V. Sowmya, and K. P. Soman, "A comparative evaluation of decomposition methods based on pitch estimation of piano notes," in *Proc. 4th Int. Conf. Smart Comput. Informat*, vol. 1, 2021, pp. 833–843.

[52] P. Adarsh, P. K. Indukala, and B. Hariharan, "An adaptive thresholding framework for detecting the subsurface movements in landslide-prone sites," in *Proc. 3rd Int. Conf. Pervasive Comput. Social Netw. (ICPCSN)*, Jun. 2023, pp. 1502–1507.

[53] G. Papazafeiropoulos and V. Plevris, "OpenSeismoMATLAB: A new open-source software for strong ground motion data processing," *Heliyon*, vol. 4, no. 9, Sep. 2018, Art. no. e00784.

[54] U.S. Geological Surv. (2023). *M5.3—6km Wnw of Toms Place*. [Online]. Available: https://earthquake.usgs.gov/earthquakes/eventpage/us2000hd8v/map

[55] *Rainfall Data of Sikkim*. Accessed: May 5, 2024. [Online]. Available: http://sikenvis.nic.in/Database/Rainfall_4227.aspx#

[56] H. Thirugnanam, M. V. Ramesh, and V. P. Rangan, "Enhancing the reliability of landslide early warning systems by machine learning," *Landslides*, vol. 17, no. 9, pp. 2231–2246, Sep. 2020.

[57] M. Sudheer, "Wireless sensor network for disaster monitoring," in *Wireless Sensor Networks: Application—Centric Design*. Rijeka, Croatia: InTech, 2010, doi: 10.5772/13119.

[58] P. Pradeep, S. Krishnamoorthy, R. K. Pathinarupothi, and A. V. Vasilakos, "Leveraging context-awareness for Internet of Things ecosystem: Representation, organization, and management of context," *Comput. Commun.*, vol. 177, pp. 33–50, Sep. 2021.

[59] C. Abancó, M. Hurlimann, B. Fritschi, C. Graf, and J. Moya, "Transformation of ground vibration signal for debris-flow monitoring and detection in alarm systems," *Sensors*, vol. 12, no. 4, pp. 4870–4891, Apr. 2012.

[60] M. Hurlimann, C. Abancó, and J. Moya, "Rockfalls detached from a lateral moraine during spring season. 2010 and 2011 events observed at the rebaixader debris-flow monitoring site (Central pyrenees, Spain)," *Landslides*, vol. 9, no. 3, pp. 385–393, Sep. 2012.

[61] A. M. Zambrano, I. Perez, C. Palau, and M. Esteve, "Technologies of Internet of Things applied to an earthquake early warning system," *Future Gener. Comput. Syst.*, vol. 75, pp. 206–215, Oct. 2017.

[62] Q. A. Gian, D.-T. Tran, D. C. Nguyen, V. H. Nhu, and D. Tien Bui, "Design and implementation of site-specific rainfall-induced landslide early warning and monitoring system: A case study at nam dan landslide (Vietnam)," *Geomatics, Natural Hazards Risk*, vol. 8, no. 2, pp. 1978–1996, Dec. 2017.

[63] M. Klapez, C. A. Grazia, S. Zennaro, M. Cozzani, and M. Casoni, "First experiences with earthcloud, a low-cost, cloud-based IoT seismic alert system," in *Proc. 14th Int. Conf. Wireless Mobile Comput., Netw. Commun. (WiMob)*, Oct. 2018, pp. 262–269.

[64] H. Tariq, F. Touati, M. A. E. Al-Hitmi, D. Crescini, and A. Ben Mnaouer, "A real-time early warning seismic event detection algorithm using smart geo-spatial bi-axial inclinometer nodes for Industry 4.0 applications," *Appl. Sci.*, vol. 9, no. 18, p. 3650, Sep. 2019.

[65] J. Fu, Z. Li, H. Meng, J. Wang, and X. Shan, ''Performance evaluation of low-cost seismic sensors for dense earthquake early warning: 2018–2019 field testing in Southwest China,'' *Sensors*, vol. 19, no. 9, p. 1999, Apr. 2019.
[66] C. Peng, P. Jiang, Q. Chen, Q. Ma, and J. Yang, ''Performance evaluation of a dense MEMS-based seismic sensor array deployed in the sichuan-yunnan border region for earthquake early warning,'' *Micromachines*, vol. 10, no. 11, p. 735, Oct. 2019.
[67] L. D'Errico, F. Franchi, F. Graziosi, A. Marotta, C. Rinaldi, M. Boschi, and A. Colarieti, ''Structural health monitoring and earthquake early warning on 5G uRLLC network,'' in *Proc. IEEE 5th World Forum Internet Things (WF-IoT)*, Apr. 2019, pp. 783–786.
[68] J. Faillettaz, M. Funk, J. Beutel, and A. Vieli, ''Towards early warning of gravitational slope failure with co-detection of microseismic activity: The case of an active rock glacier,'' *Natural Hazards Earth Syst. Sci.*, vol. 19, no. 7, pp. 1399–1413, Jul. 2019.
[69] K. Fauvel, D. Balouek-Thomert, D. Melgar, P. Silva, A. Simonet, G. Antoniu, A. Costan, V. Masson, M. Parashar, I. Rodero, and A. Termier, ''A distributed multi-sensor machine learning approach to earthquake early warning,'' in *Proc. AAAI Conf. Artif. Intell.*, vol. 34, no. 1, 2020, pp. 403–411.
[70] K. K. Khedo, Y. Bissessur, and D. S. Goolaub, ''An inland wireless sensor network system for monitoring seismic activity,'' *Future Gener. Comput. Syst.*, vol. 105, pp. 520–532, Apr. 2020.
[71] R. M. Allen, Q. Kong, and R. Martin-Short, ''The MyShake platform: A global vision for earthquake early warning,'' *Pure Appl. Geophys.*, vol. 177, no. 4, pp. 1699–1712, Apr. 2020.
[72] M. Elmoulat, O. Debauche, S. Mahmoudi, S. A. Mahmoudi, P. Manneback, and F. Lebeau, ''Edge computing and artificial intelligence for landslides monitoring,'' *Proc. Comput. Sci.*, vol. 177, no. 1, pp. 480–487, Jun. 2020.
[73] M. Gamperl, J. Singer, and K. Thuro, ''Internet of Things geosensor network for cost-effective landslide early warning systems,'' *Sensors*, vol. 21, no. 8, p. 2609, Apr. 2021.
[74] Z. Li, L. Fang, X. Sun, and W. Peng, ''5G IoT-based geohazard monitoring and early warning system and its application,'' *EURASIP J. Wireless Commun. Netw.*, vol. 2021, no. 1, pp. 1–16, Dec. 2021.
[75] A. Makama, K. Kuladinithi, and A. Timm-Giel, ''Wireless geophone networks for land seismic data acquisition: A survey, tutorial and performance evaluation,'' *Sensors*, vol. 21, no. 15, p. 5171, Jul. 2021.
[76] Q.-M. Xie, K. Long, Z.-M. Li, L.-C. Chen, H. Liu, H. Xu, F. He, D. Liang, X.-K. Xiang, and Q. Ma, ''Stability evaluation for steep bank slope with microseismic monitoring in three Gorges reservoir area,'' *J. Mountain Sci.*, vol. 19, no. 6, pp. 1588–1601, Jun. 2022.
[77] C.-M. Yang, J.-M. Chang, C.-Y. Hung, C.-H. Lu, W.-A. Chao, and K.-H. Kang, ''Life span of a landslide dam on mountain valley caught on seismic signals and its possible early warnings,'' *Landslides*, vol. 19, no. 3, pp. 637–646, Mar. 2022.
[78] R. Dhanagopal and B. Muthukumar, ''A model for low power, high speed and energy efficient early landslide detection system using IoT,'' *Wireless Pers. Commun.*, vol. 117, no. 4, pp. 2713–2728, Apr. 2021.

P. K. INDUKALA received the bachelor's degree in information technology from Cochin University of Science and Technology and the master's degree in computational engineering and networking from Amrita Vishwa Vidyapeetham, Coimbatore. She is currently a Research Associate with the Center for Wireless Networks and Applications, Amrita Vishwa Vidyapeetham. She has more than nine years of experience working on different research projects funded by organizations, such as the Ministry of Earth Sciences (MoES) and the Department of Science and Technology (DST), Government of India. Her research interests include the Internet of Things, signal processing, machine learning, computational optimization, and deep learning.

U. G. GOSH received the bachelor's degree in electronics and communication engineering from Amrita Vishwa Vidyapeetham. He is currently a Project Associate with the Center for Wireless Networks and Applications, Amrita Vishwa Vidyapeetham. He has more than 12 years of experience working on different research projects funded by organizations, such as the Ministry of Earth Sciences (MoES), and the Government of India. His interests include embedded system development and the Internet of Things.

MANEESHA VINODINI RAMESH (Senior Member, IEEE) received the Ph.D. degree in computer science and engineering from Amrita Vishwa Vidyapeetham, in 2009, where she is currently the Provost, Strategic Initiatives, Research and Innovation, Interdisciplinary, International, and AI+X. She also holds the positions of the Director of Amrita Center for Wireless Networks, the Dean of International Programs, the Dean of the School for Sustainable Development, and the UNESCO Chair of experiential learning for Sustainable Innovation and Development, School for Sustainable Development. She is listed among the top two scientists in the world by an index made by Stanford University, in 2021. She has more than 200 articles, including several journals and best paper awards. She has given invited talks at several eminent universities all over the world. She is also the Co-Principal Investigator of European Commission funded Wireless Sensor Networks with Self Organization Capabilities for Critical and Emergency Applications (WINSOC) Project and the Principal Investigator of eight internationally recognized projects funded by different organizations from all over the world. In 2012, she received the NABARD Award for Rural Innovation 2nd prize from the Honorable Finance Minister, Government of India, for her research activities that benefited the rural community. She served as the Program Chair for ACWR 2011. She is an Editor of the Ad Hoc Networks Elsevier.